Ion-Induced Nucleation of Dibutyl Phthalate Vapors on Spherical and Nonspherical Singly and Multiply Charged Polyethylene Glycol Ions

Albert G. Nasibulin,*,† Juan Fernandez de la Mora,‡ and Esko I. Kauppinen†,§

NanoMaterials Group, Laboratory of Physics and Center for New Materials, Helsinki University of Technology, P.O. Box 1000, 02044 VTT, Espoo, Finland, Mechanical Engineering, Yale University, P.O. Box 208286, New Haven, Connecticut 06520-8286, and VTT Biotechnology, P.O. Box 5100, 02150, Espoo, Finland

Received: July 17, 2007; In Final Form: November 7, 2007

Dibutyl phthalate vapor nucleation induced by positive polyethylene glycol (PEG) ions with controlled sizes and charges was experimentally studied. The ions were produced by electrospray ionization, classified in a high-resolution differential mobility analyzer, and studied in a nano condensation nucleus counter of the mixing type. Ionic radii of PEG varied from 0.52 to 1.56 nm, including from singly to quadruply charged ions. Some of these ions are fully stretched chains, other are spherical, and others have intermediate forms, all of them having been previously characterized by mobility and mass spectrometry studies. Activation of PEG_{1080}^{+2} requires a supersaturation almost as high as that required for small singly charged ions and higher than for PEG_{1080}^{+}. This anomaly is explained by the Coulombic stretching of the ion into a long chain, where the two charged centers appear to be relatively decoupled from each other. The critical supersaturation for singly charged spherical ions falls below Thomson's (capillary) theory and even below the already low values seen previously for tetraheptyl ammonium bromide clusters. Spherical PEG_{4120}^{+2} falls close to the Thomson curve. The trends observed for slightly nonspherical PEG_{4120}^{+3} and highly nonspherical (but not quite linear) PEG_{4120}^{+4} are intermediate between those of multiply charged spheres and small singly charged ions.

1. Introduction

Although ion-induced nucleation has been studied for over a century, many unknowns do still cloud our understanding of the phenomenon. One of the reasons is experimental, since control of both the ion and the thermodynamic state of the condensing vapor involved has been difficult to obtain. Considerable success at overcoming this problem has been achieved by Kane and colleagues[1−3] by resonant photoionization of vapor species inside a cloud chamber. This technique has enabled the measurement of critical supersaturations for a variety of vapor-ion combinations. However, it is restricted to positively singly charged and small ions, which represents a serious limitation of the principal variables in classical heterogeneous nucleation theories (the size, the sign and the number of charges of the nucleating particle). Ion-induced nucleation studies of larger and involatile ions of almost continuously variable diameters have been made possible more recently via electrospray (ES) ionization.[4] Since a wide range of cluster ions is produced by this method, it is necessary to purify this complex mixture before introducing it into a well characterized supersaturated vapor. This ion-cleaning step was first demonstrated by Seto et al.[5] with a high-resolution differential mobility analyzer (DMA), which combines a flow field and an electric field to separate ions in space according to their electrical mobility, and hence yields a steady stream of monomobile ions at atmospheric pressure. They found a critical supersaturation for the initiation of nucleation on singly charged cations smaller than predicted by Thomson's model, whereas doubly charged ions were very close to the Thomson's curve. However, their values for the critical supersaturation depended on an unreliable assumption of adiabatic mixing.[6] Further investigations of nucleation on mobility-selected ions were carried out by Gamero-Castaño and Fernandez de la Mora, with an improved version of the instrument producing the supersaturated state, and a reliable value of the supersaturation.[6] They were able to measure critical supersaturations on singly charged salt clusters from 0.94 to 2.97 nm in diameter, as well as singly and multiply charged protein ions of a few nm in diameter.[7−8] They found fair agreement with Thomson's critical supersaturation for singly charged particles. However, at higher charge states, they saw a much weaker effect of the charge than expected from classical theory.

In the present paper, we investigate ion-induced nucleation on polyethylene glycol (PEG) ions, formed by electrospray ionization, and purified with the help of a high-resolution DMA. The PEG ions have the useful advantage of permitting a relatively fine and discrete variation of the ion size. ES ionization also produces these ions in relatively high initial charge states, which may be reduced by partial neutralization, providing a relatively wide control of the ion charge state introduced in the supersaturated vapor. In an earlier study,[9] the conformation of naturally charged PEG ions was found to be linear (fully stretched), whereas that of ions of mass m and charge ne such that m (amu) $> 500n^2$ is rather compact and approximately describable as a sphere of constant density.[10] These findings warranted further the investigation of ion-induced nucleation of PEG ions as a function of their mass and charge, covering conditions where they are spherical, as well as those where they become increasingly stretched.

* Author to whom all correspondence should be addressed. E-mail: albert.nasibulin@hut.fi.
† Helsinki University of Technology.
‡ Yale University.
§ VTT Biotechnology.

10.1021/jp0755995 CCC: $40.75 © 2008 American Chemical Society
Published on Web 01/24/2008

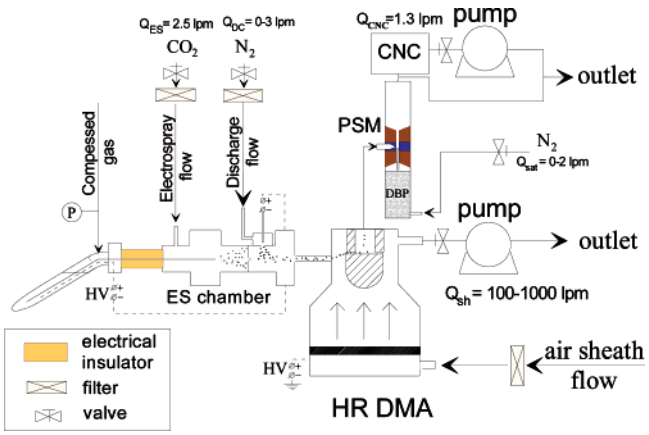

Figure 1. Schematic of the experimental setup.

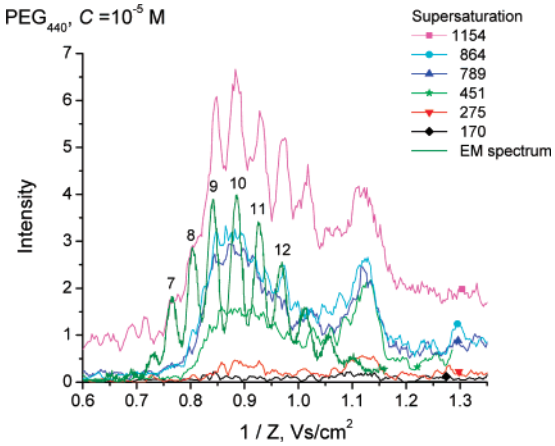

Figure 2. Mobility spectra of charged PEG_{440} ions at different supersaturations of DBP vapor. The numbers above the peaks indicate the number of ethylene glycol groups in the PEG chain. A spectrum obtained at $S = 1154$ corresponds to the onset of homogeneous dibutyl phthalate vapor nucleation.

2. Experimental Section

Materials. Dibutyl phthalate has been used as a source of vapor for these nucleation studies. The heterogeneous charged centers were introduced from three kinds of PEG samples, all having relatively narrow mass distributions ($\Delta m/m$ less than 0.15), nominally centered at molecular weights of 440, 1080, and 4120 Da (Polymer laboratories, Amherst, MA). Solutions containing 10^{-6} to 5×10^{-5} mol/L PEG sample and 0.02 mol/L ammonium acetate were freshly prepared in deionized water. The ammonium acetate serves the purpose of providing sufficient electrical conductivity for the sprayed drops to be very small from birth, facilitating the production of drops containing only one sample molecule.[11] For ion mobility calibration at fixed experimental conditions, the standard solution containing tetraheptyl ammonium ions (1 mmol/L in propanol), with the reference mobility value of $Z_{(C_7H_{15})_4N^+} = 0.962$ cm^2/V/s, was used.[6] As carrier gases to produce an electrospray and to partially neutralize multiply charged particles, carbon dioxide and nitrogen of industrial purity were respectively used. Filtered room air was utilized as a sheath flow through the DMA.

Experimental Setup. The experimental setup is shown in Figure 1. Charged PEG particles were generated by electrospray ionization. A PEG sample solution was placed in a capsule. Using hand-compressed room air, the liquid was pushed through a silica capillary (20 μm ID; Polymicro Technologies) from the capsule into the electrospraying end of the capillary in the ES chamber. The formed spray particles were carried in the surrounding stream of carbon dioxide, where the solvent evaporated and produced ions of solute species. Earlier work has shown that electrosprayed PEG ions in ammonium acetate buffer are formed by attachment of one or several ammonium ions, $PEG(NH_4)^+_n$.[9] Since the PEG_{4120} sample produces only multiply charged particles, this spray was partially neutralized. For this purpose, the PEG_{4120} ions were mixed turbulently in a separate chamber with a nitrogen stream bringing negative ions from an adjacent chamber, where a corona discharge was established through a potential difference between a centered steel needle and the chamber walls. Variation of the corona current or the flow rates of corona gas enabled controlling the charge state of the particles.

The positively charged residue particles containing a PEG molecule and one or more ammonium ions were introduced in a differential mobility analyzer (DMA).[12,13] The unusually high resolution of this instrument follows from an ability to operate laminarly at Reynolds numbers up to 30 000, at flow rates in excess of 1000 L/min. The sheath air flow was filtered upstream of the DMA by means of a HEPA filter from a household vacuum cleaner (Eureka, style HF1). The classified monodisperse particles were introduced into a region of controlled supersaturation in an instrument previously described by Gamero-Castaño and Fernandez de la Mora.[14] It is based on a simple modification of the particle size magnifier (PSM) developed by Okuyama and colleagues[15] and will be denoted here as the PSM. Briefly, pure nitrogen is introduced into a heated saturator containing a bed of silica gel impregnated with DBP. This vapor is then driven through a heated conduit (assuring the absence of vapor losses) into an externally cooled mixing chamber, where the hot vapor is mixed turbulently with the cold flow of air carrying mobility-selected PEG ions. Prior thermocouple measurements by Gamero-Castaño have established that the mixing temperature is within one or two degrees of the cold wall temperature. The supersaturation was therefore approximated here as that corresponding to the known vapor flux from the saturator, diluted by the known flow rate of air, at the temperature of the cold wall (measured here with a thermocouple). This temperature was essentially constant and equal to 286 K for all the experiments. We used the physicochemical properties of DBP reported by Seto et al.[5] The nuclei formed in this region grew then into a detectable size range and were identified individually by TSI's CPC, model 3760, (St. Paul, MN; detection size limit $\sim$ 10 nm). The supersaturation of DBP vapors was varied by changing the saturator temperature and the nitrogen flow rates (in the range of 0−2 L/min). After the PSM, a part of the gaseous flow was extracted and directed into the particle counter, wherein the flow rate was always maintained at the constant value of 1.3 L/min.

Experimental Results. Figures 2 and 3 show the signal in the detector (proportional to the number of ions nucleated) as a function of the inverse ion mobility, Z. The various curves correspond to different supersaturations in the PSM, for 10^{-5} M solutions of PEG_{440} and PEG_{1080}. These spectra are obtained by fixing all temperatures and flow rates, and varying the voltage difference V between the two DMA electrodes. The measured voltages are directly proportional to the inverse mobility, through a constant determined by running a sample with a known mobility standard. As one can see from Figures 2 and 3, the DMA resolves individual m-mers of PEG molecules, which were registered by the PSM. The assignment of the numbers of charges and ethylene glycol groups in ions was carried out on the basis of mass spectrometry measurements of mobility selected PEG molecules in a wide range of charges and masses

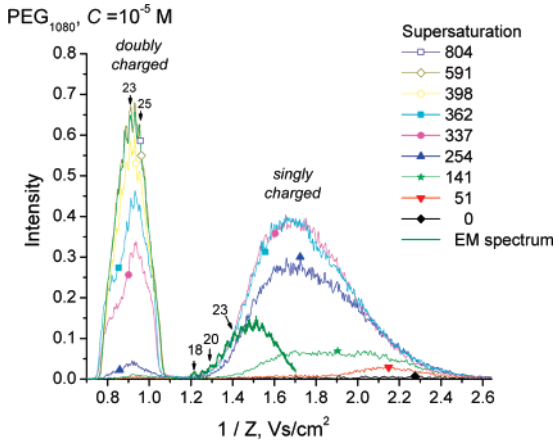

Figure 3. Nano CNC signal of naturally charged positive ions from PEG_{1080} solution versus inverse mobility at different DPB vapor supersaturations. The numbers above the peaks indicate the number of ethylene glycol groups in each PEG molecule.

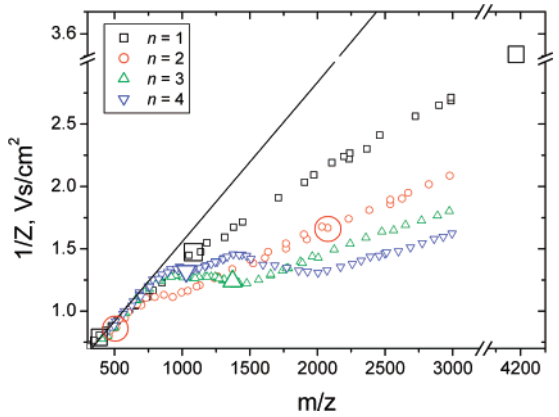

Figure 4. Shape of the clusters studied revealed by insertion in the inverse mobility versus mass data of ref 9 (small and large symbols) and the present study, respectively. The common asymptote on the lower left, marked with a line, corresponds to fully stretched chains. The separate straight pieces to the right correspond to spheres.

reported in ref 9 and reproduced in Figure 4. The number of charges, n, and mass of the molecule can be calculated taking into account the numbers of ammonium ions and ethylene glycol groups, m, respectively

$$H(OCH_2CH_2)_mOH(NH_4^+)_n; \quad \{n = 1, 2, 3, 4\}$$

We have also reported high-resolution spectra for PEG_{440} and PEG_{1080} obtained with the help of an electrometer (EM) detector.[16] It is worth noting that some of these results are corrected here according to reference.[9] Namely, for singly charged samples ref 16 contained incorrect assignment of three ethylene glycol groups less for each of the peaks. The EM spectra allow us to correlate all ion mobilities to the certain number of ethylene glycol groups contained in an ion. Note that the singly charged peak of PEG_{1080} includes an unknown contaminant in the range 1.2−1.3 Vs/cm^2. Nonetheless, the relevant data for the ion-induced nucleation of singly charged PEG_{1080} ions can be obtained in the range of $1/Z$ from about 1.3 to about 1.7.

Mobility spectra of a partially neutralized PEG_{4120} sample are shown in Figure 5, each curve corresponding again to a different supersaturation in the PSM. The various broad peaks on the spectra correspond to different charge states. Electrospray ionization is known to produce charge states that increase with the molecular mass of the ion. This is consistent with our

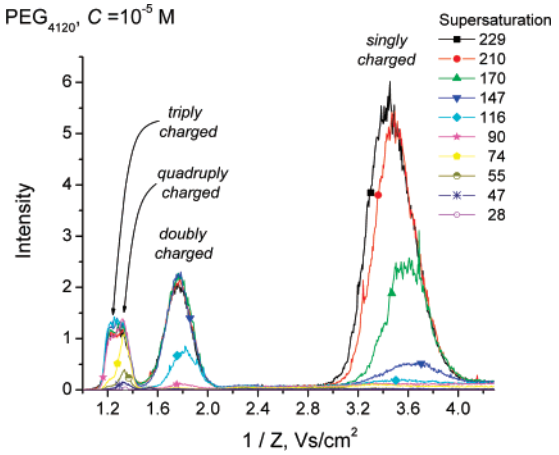

Figure 5. Mobility spectra of charged PEG_{4120} ions at different supersaturations of DBP vapor.

observation that the smallest polymer sample PEG_{440} (containing approximately 7 ethylene glycol groups) yields only singly charged particles. PEG_{1080} (about 25 ethylene glycol groups) produces singly and doubly charged ions, whereas PEG_{4120} (about 92 monomer groups) carries up to four charges. In Figure 5, one sees two different ions activating at different supersaturations in the region centered at $1/Z = 1.3$ V s/cm^2. The corresponding ions can be assigned to PEG_{4120}^{+3} and PEG_{4120}^{+4} based on the data in Figure 4 (large green up triangle at $1/Z = 1.24$ and large blue down triangle at 1.32 V s/cm^2, respectively). Note that the least mobile ion has the highest charge, an irregularity following from substantial stretching of the quadruply charged ion.[9]

On the basis of the spectra obtained at different supersaturations S (ratio between the actual partial pressure of DBP and its equilibrium vapor pressure: $S = P/P^0$), we can infer the critical supersaturation S^* for the activation of each of the PEG ions. The experimental value of S^* is defined as the value of S at which half of the ions are activated. As seen in Figure 6, the ion signal curve $I(S)$ rises very sharply with S from zero to a maximum value in a narrow range of S. This saturation effect is also clearly shown in Figure 5, where the mobility spectra corresponding to various S coincide with each other exactly at either large S or large $1/Z$, when the activation probability tends to unity. Because of the narrow transitions seen in Figure 6, the value S^* of S at half-height is relatively well defined, even when the value of the detector signal corresponding to 100% activation may be slightly ambiguous in some cases. In particular, the 100% activation limit is closely approached but not fully attained in Figure 2 due to interference of homogeneous nucleation at the largest S studied ($S = 1154$). This interference is obvious from the fact that a constant background of particles is seen, even at voltages where there are no ions. The critical supersaturation measured for homogeneous nucleation of DBP vapor at the experimental temperature of 286 K is 1010, very close to that reported by Hämeri and Kulmala in a laminar flow diffusion chamber.[17]

Mobilities, ionic radii (estimated from the masses and density) and corresponding critical supersaturations needed for the activation of ions are gathered in Table 1. For these calculations we have adopted the same density, $\rho = 1130$ kg/m^3, previously used in reference.[9]

3. Discussion

In order to compare the experimental results with the classical theory, let us present our data in the framework of Thomson's

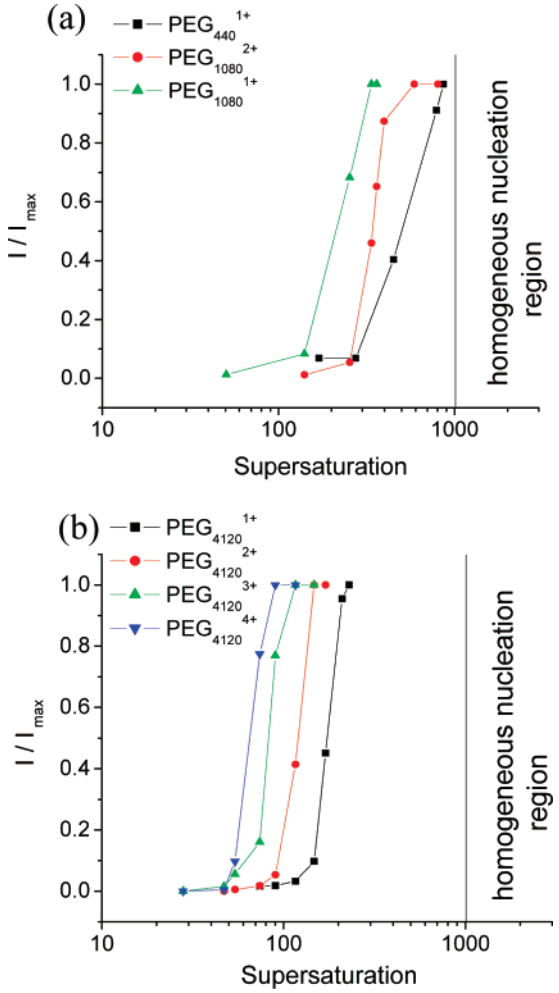

Figure 6. Effect of DBP vapor supersaturation on the activation probability of (a) naturally charged ions from PEG_{440} and PEG_{1080}; (b) charge-reduced PEG_{4120} ions.

model. Considering an ideal system consisting of ions in the atmosphere of supersaturated vapor, one can show[5] that the free energy change during the formation a droplet on the surface of a preexisting ion of radius a can be written as

$$\Delta G(T,P) = 4\pi r^2\sigma - \frac{4\pi}{3V} r^3 kT \ln S - \frac{(ne)^2(1-1/\epsilon)}{8\pi\epsilon_0}\left(\frac{1}{a}-\frac{1}{r}\right) \quad (2)$$

where σ is the surface tension, V is the molecular volume, and ϵ is the dielectric constant of the liquid surrounding the ion. The condition of metastable equilibrium, when the critical embryo is formed, can be presented as

$$\left(\frac{\partial \Delta G}{\partial r}\right)_{T,P} = 0 = 8\pi r\sigma - \frac{4\pi}{V} r^2 kT \ln S - \frac{(ne)^2(1-1/\epsilon)}{8\pi\epsilon_0 r^2} \quad (3)$$

For further analysis of eq 3, let us introduce the Rayleigh radius r_R

$$r_R^{\,3} = \frac{(ne)^2(1-1/\epsilon)}{64\pi^2\epsilon_0\sigma} \quad (4)$$

TABLE 1: Mobilities, Number of Ethylene Glycol Groups, Ionic Radii (Estimated from Masses and Density) and Corresponding Critical Supersaturations Needed for Ion Activation

	1/Z, Vs/cm^2	r, nm	S^*
PEG_{440}	0.808	0.507	602
singly	0.840	0.576	502
charged	0.884	0.539	453
PEG_{1080}	1.408	0.738	221
singly	1.484	0.761	227
charged	1.559	0.784	214
	0.806	0.843	323
PEG_{1080}	0.833	0.870	339
doubly	0.911	0.870	344
charged	0.961	0.870	328
	1.008	0.898	323
	3.906	1.386	148
PEG_{4120}	3.704	1.343	157
singly	3.597	1.322	162
charged	3.497	1.300	172
	2.101	1.447	94
	2.049	1.427	97
	2.000	1.406	100
	1.949	1.386	104
PEG_{4120}	1.927	1.375	106
doubly	1.901	1.365	111
charged	1.848	1.343	118
	1.799	1.322	121
	1.751	1.300	123
	1.701	1.278	125
	1.650	1.255	127
	1.600	1.232	129
PEG_{4120}	1.200	1.447	58.7
triply	1.170	1.417	61.7
charged	1.140	1.386	69.8
PEG_{4120}	1.401	1.564	84.1
quadruply	1.350	1.541	85.2
charged	1.300	1.518	85.4

equal when ϵ tends to infinity to the minimum radius that a droplet of charge ne can take without breakup, and the Kelvin radius

$$r_K = \frac{2\sigma V}{kT \ln S} \quad (5)$$

Then, eq 3 can be rewritten as

$$1 - \frac{r_R^{\,3}}{r^3} = \frac{r}{r_K} \quad (6)$$

or in dimensionless form as[5]

$$1 - x^{-3} = \alpha x \quad (7)$$

where x is the reduced radius, $x = r/r_R$, and α is a rescaled supersaturation

$$\alpha = \frac{r_R}{r_k} = \frac{r_R kT}{2\sigma V} \ln S \quad (8)$$

Below a critical supersaturation, $\alpha < \alpha^* = 0.472$, eq 7 has two solutions associated to two extrema: a minimum at $x < 1.587$ (corresponding to a stable solvated ion), and a maximum at $x > 1.587$. At the critical condition $\alpha = 0.472$, the minimum and the maximum merge into an inflexion point at $x = 1.587$. All ions smaller than this critical size are activated (grow from their small initial dimensions to macroscopic sizes) at this critical

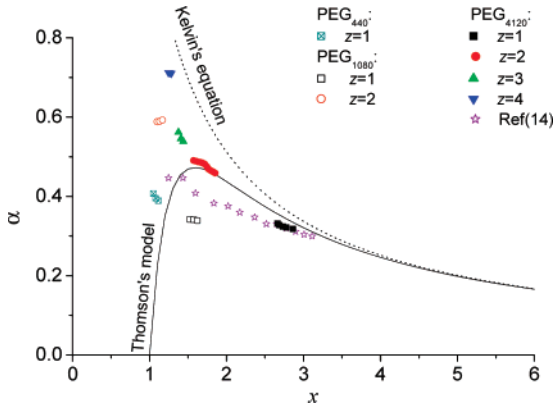

Figure 7. Thomson's dimensionless relation between critical supersaturation and ion radius.

supersaturation, independently of their size. Ions larger than this critical size are activated at a supersaturation $\alpha(x) < \alpha^*$, defined by the descending part of the line labeled Thomson curve in Figure 7. This branch merges at larger sizes ($x \gg 1$) with the Kelvin curve (appropriate for heterogeneous nucleation on uncharged particles).

Figure 7 shows also a comparison of the experimental results with the predictions of classical ion-induced nucleation (Thomson's model) and heterogeneous nucleation on a neutral drop (Kelvin's equation). For reference the figure includes also literature data[14] on singly charged tetraheptyl ammonium bromide clusters. Some qualitative agreement is found with Thomson's model and the earlier measurements[14] for singly charged PEG ions in the form of a substantial reduction in α below the Kelvin curve. However, a large discrepancy is observed for the multiply charged PEG ions. This discrepancy increases with the charge state of the ions, with a tendency to approach the Kelvin curve, as if the effect of the charge tended to disappear, as previously observed with multiply charged proteins.[14] An even more peculiar effect seen in Figure 6a is that the critical supersaturation needed for the activation of doubly charged PEG_{1080} ions is higher than that for the singly charged ions. Yet, classical theory for spherical particles predicts exactly the opposite: the higher the charge state, the smaller the critical supersaturation for the activation of an ion of given size. Part of the unexpected effect of the charge on the value of the critical supersaturations can be explained as due to charge-induced conformational change of the ion. Indeed, electrical mobility studies of mass-selected PEG particles reported by Ude et al.[9] reveal the existence of a multitude of uncharacterized shapes between two well-defined limits corresponding to either essentially spherical ions (for m(amu) $< 500z^2$) or fully stretched chains. In particular, singly charged PEG_{440} and PEG_{1080} ions have spherical structures as can be seen from Figure 4. However, doubly charged PEG_{1080} ions can be seen in Figure 4 to fall in the fully stretched region. It is interesting to see that the critical supersaturation for PEG_{1080}^{+2} is relatively close (in logarithmic coordinates for S) to that of PEG_{1080}^{+1}. To first approximation, then, the charges on this stretched chain are sufficiently distant from each other to behave as if they were independent ions of small dimensions. The data for PEG_{1080}^{+2} should then be plotted as for small singly charged ions by dividing by $2^{2/3}$ the experimental value shown in the figure ($\alpha = 0.59$): $\alpha = 0.59/2^{2/3} = 0.37$. This value is smaller than the classical nucleation prediction for small ions, $a^* = 0.472$, but it is in line with the other data shown in Figure 7 for singly charged ions. The retrograde behavior seen is therefore explainable in terms of shape effects. Note however that the datum for PEG_{1080}^{+2} interpreted as two isolated singly charged ions and our two other data for singly charged PEG ions fall clearly below the Thomson curve, as well as below the tetraheptyl ammonium cluster series.

Singly and doubly charged PEG_{4120} ions fall within the spherical shape region of ref 9. Both appear reasonably close to the Thomson curve, but the doubly charged ion falls well above the singly charged PEG series. Triply charged PEG_{4120} ions are relatively close to the critical condition for loss of sphericity but with a mobility about 10% smaller than that of a spherical ion of the same mass. For an ellipsoidal geometry, this represents a substantial nonsphericity. Hence this ion has a clear non-spherical shape, but it is also very far from a linear fully stretched chain. Quadruply charged PEG_{4120} ions are much further from spherical but still relatively far also from fully stretched. The corresponding critical supersaturations are intermediate from those corresponding to singly charged ions (fully stretched limit) and spherical ions (Thomson curve), so pending a more realistic theory introducing shape effects, no contradiction with classical theory is evident.

4. Conclusions

Ion-induced nucleation of dibutyl phthalate vapor was experimentally studied. Vapor nucleation was induced by positively charged polyethylene glycol ions with controlled charge and mass. The ions were produced by electrospray ionization, classified in a high resolution differential mobility analyzer, and studied in a nano condensation nucleus counter of the mixing type. The mass diameter of PEG varied from 0.52 to 1.56 nm, and its charge state from $n = +1$ to $n = +4e$. An anomalous increase in critical supersaturation resulting from addition of one charge to PEG_{1080} can be explained in terms of strong Coulombic stretching of the polymer chain, which makes each of the two ions behave similarly as if they were two separate singly charged entities. A serious departure from classical theory predictions is seen for PEG_{4120}^{+2} and PEG_{4120}^{+4}, similarly as found earlier for protein ions. However, because these two PEG_{4120} ions are considerably non-spherical (unlike in previous protein work) this finding here is not necessarily paradoxical.

Acknowledgment. This work was supported by the Academy of Finland and the European Community Research Training Network "Nanocluster" Grant No. HPRN-CT-2002-00328. Financial support from the U.S. National Science Foundation, Grant CTS-9871885, is gratefully acknowledged.

References and Notes

(1) Kane, D.; Fisenko, S.; El-Shall, M. S. *Chem. Phys. Lett.* **1997**, *277*, 6.

(2) Kane, D.; Daly, G. M.; El-Shall, S. *J. Phys. Chem.* **1995**, *99*, 7867.

(3) Kane, D.; El-Shall, S. *Chem. Phys. Lett.* **1996**, *259*, 482.

(4) Banks, J. F., Jr.; Shen, S.; Whitehouse, C. M.; Fenn, J. B. *Anal. Chem.* **1994**, *66*, 406.

(5) Seto, T., Okuyama, K.; de Juan, L.; Fernandez de la Mora, J. *J. Chem. Phys.* **1997**, *107*, 1576.

(6) Gamero-Castaño, M.; J. Fernández de la Mora, *Anal. Chim. Acta* **2000**, *406*, 67.

(7) Gamero-Castaño, M. *The transfer of ions and charged nanoparticles from solution to the gas phase in electrosprays*. Ph.D. Thesis, Yale University: New Haven, CT, 1999.

(8) Gamero-Castaño, M.; Fernández de la Mora, J. *J. Chem. Phys.* **2002**, *117*, 3345.

(9) Ude, S.; Fernández de la Mora, J.; Thomson, B. A. *J. Am. Chem. Soc.* **2004**, *126*, 12184.

(10) Saucy, D.; Ude, S.; Lenggoro, W.; Fernandez de la Mora, J. *Anal. Chem.* **2004**, *76*, 1045.

(11) Kaufman, S. L.; Dorman, F. D. *J. Aerosol Sci.* **1999**, *30*, S555.

(12) Eichler, T. *A DMA for ions and nanoparticles: laminar flow at high Reynolds numbers*. Senior Graduation thesis, Fachhochschule Offenburg, Germany, 1997.

(13) Fernandez de la Mora, J.; de Juan, L.; Eichler, T.; Rosell, J. *Trends Anal. Chem.* **1998**, *17*, 328.

(14) Gamero-Castaño, M.; Fernández de la Mora, J. *J. Aerosol Sci.* **2000**, *31*, 757.

(15) Okuyama, K.; Kousaka, Y.; Motouchi, T. *Aerosol Sci. Technol.* **1984**, *3*, 353.

(16) Nasibulin, A. G.; Kauppinen, E. I.; Thomson, B. A.; Fernandez de la Mora, J. *J. Nanopart. Res.* **2002**, *4*, 449.

(17) Hämeri, K.; Kulmala, M. *J. Chem. Phys.* **1996**, *105*, 7696.